Desalination and Water Treatment
www.deswater.com

1944-3994 / 1944-3986 © 2011 Desalination Publications. All rights reserved.
doi: 10.5004/dwt.2011.1614

25 (2011) 176–186
January

Mutual action of copper (II) and a nonionic surfactant (oxyethylated alcohols) on their simultaneous removal by a neutral hyper-cross-linked polystyrene adsorbent

Danutė Kaušpėdienė*, Aušra Selskienė

Institute of Chemistry, A.Goštauto 9, 01108 Vilnius, Lithuania
Tel.+370 (5) 2648843; Fax +370 (5) 2649774; email: dana@ktl.mii.lt

Received 30 October 2009; Accepted in revised form 3 June 2010

ABSTRACT

The mutual action of Cu(II) and nonionic surfactant Lutensol AO-10 on their sorption onto neutral hyper-cross-linked polystyrene Macronet MN-200 from mixtures has been investigated by the analysis of sorption equilibrium and kinetic data. The experimental equilibrium data were analyzed using the Langmuir and Freundlich models. The sorption mechanism of Cu(II) from one-component solutions or Cu(II) and AO-10 from their mixture corresponded to the Langmuir model rather than to the Freundlich one, whereas the sorption mechanism of AO-10 from one-component solutions proceeded according to the Freundlich rather than to the Langmuir model. The pseudo-second-order-reaction and intraparticle diffusion models (Weber–Morris plot) were used to describe the sorption kinetics, and to determine the sorption rate (k_2), intraparticle (k_i) and external diffusion (k_s) constants. The k_2 values obtained for Cu(II) sorption from solutions free from AO-10 was higher than those obtained for sorption from solutions free from Cu(II). The presence of AO-10 in the mixture results in a decrease in k_2 value for Cu(II), whereas the presence of Cu(II) leads to an increase in k_2 value determined for AO-10. The Cu(II) sorption rates from the solution free from AO-10 or Cu(II) and AO-10 from their mixture are dependent on intraparticle and external diffusion proceeding simultaneously. The sorption rate of AO-10 from one-component solution is limited only by intraparticle diffusion. Electron microscopy (SEM) images of MN 200 surface, scanned before and after AO-10 sorption, distribution of Cu(II) in the cross-section of the bead after Cu(II) sorption in the presence of AO-10 are in agreement with sorption measurements.

Keywords: Copper (II); Nonionic surfactant; Sorption; Hyper-cross-linked polystyrene; Environment protection

1. Introduction

Large quantities of surfactants released into the environment from variety of manufacturing processes as well as from households may result in serious health and environmental problems. Many industries use cancerous Cu(II) compounds, which has a negative impact on the water quality. To prevent the environment contamination with Cu(II) and the nonionic surfactant, the elimination of both contaminants and reuse of wastewaters are required.

Sorption onto activated carbon and the hydrogen form of the weak acid cation exchangers is one of the most attractive processes for the treatment of wastewaters, recovering water for reuse and preventing pollution of

---

* Corresponding author.

the environment with heavy metal cations and nonionic surfactant molecules [1–6]. The sorption of metal ions by activated carbon from aqueous solutions leads to the formation of complexes with the functional groups present on the carbon surface [4,5]. Whereas the nonionic surfactant may be absorbed due to the hydrophobic interaction amongst the sorbed molecules, similarly to the process occurring during micelle formation, when their concentration in the solution exceeds the limit given by the critical micelle concentration [1–3]. The sorption of metal ions from the aqueous solution by the hydrogen form of a weak acid cation exchanger proceeds either by ion exchange or complexes formation, whereas the sorption of nonionic surfactant - by the formation of the hydrogen bond between the protonated carboxyl group and hydrophilic chain ($-C_2H_4O-$ head group) of nonionic surfactant. However, there are some problems using activated carbon, e.g., its high regeneration costs and production of fines due to its brittle nature [7]. Synthetic ion exchangers, based on crosslinked polystyrene-divinilbenzene polymers, offer a relatively small surface area at a high cost. This stimulates further research for the polymeric sorbents, including the hyper-cross-linked polystyrene (sorbent of a new generation), as a neutral hydrophobic sorbent.

The hyper-cross-linked neutral polystyrene sorbents including Macronet MN 200 display an increased affinity to all kinds of volatile organic compounds in air (pentane, octane, undecane, isooctane, cyclohexane, toluene, methanol, and dichloromethane) [8]. Because of its high rigidity and pressure resistance, Macronet MN-200 is considered to be a promising stationary phase for a high performance liquid chromatography column (HPLC) for the separation of hydrophobic materials such as phenols, dialkyl phthalates and polyaromatic compounds [9]. MN 200 was also applied for the removal of organic pollutants (phenol and chlorphenols) from potable water [10]. The retention mechanism of organic pollutants may involve not only hydrophobic but also π–π interactions [9,11]. Moreover, the Macronet MN 200 also can bind the ions of heavy metals [11]. A chromatographic column, packed with MN-200, separates the mixtures of Bi^{3+} and Pb^{2+} ions, as well as the mixtures of Zn^{2+} and Cd^{2+} [11,12]. The sorption of acetates and nitrates of Hg, Pb, Ag and Bi by MN-200 from acetate buffers or nitric acid solutions proceeds by the formation of p-complexes between the metal cations and two or more benzene rings in the hyper-cross-linked polystyrene.

A novel process of size-exclusion chromatography (SEC) of concentrated solutions of simplest mineral electrolytes was performed on two samples of neutral hyper-cross-linked polystyrene Macronet MN-202 and Macronent MN-270 [13]. The selectivity of separation of two electrolytes, MeCl and HCl, was found to be determined by the difference in size of cation Me^+ and anion Cl^-, the largest ions of the two electrolytes under separation, not those two ions (Me^+ and H^+) which makes the electrolytes different from each other. Selectivity in SEC, as distinct from other types of chromatography, makes itself evident at higher concentrations of electrolytes, which was explained by exclusion of smaller species from the concentrated solution into small pores of the column packing that are inaccessible to large species.

However no literature seems to be available on the simultaneous removal of Cu(II) cations and the nonionic surfactant from wastewaters by neutral hyper-cross-linked polystyrene. The data concerning the sorption equilibrium and kinetics are required for modeling of wastewater treatment system from laboratory to large-scale equipment, for calculating the necessary amount of sorbent and the time for the sorption [14,15]. The simultaneous sorption of Cu(II) cations and the molecules of nonionic surfactant by neutral hyper-cross-linked polystyrene may be also of environmental interest with respect to the prevention of the pollution with toxic Cu(II) and the nonionic surfactant, and of industrial interest with respect to both the quality of recycled rinse water from copper plating and the quality of copper coatings.

The objective of this work was to determine the mutual action of Cu(II) and nonionic surfactant Lutensol AO-10 (oxyethylated higher fatty alcohols) on the equilibrium and kinetics of their simultaneous sorption by neutral hyper-cross-linked polystyrene Macronet MN-200.

2. Experimental

2.1. Materials

Nonionic surfactant Lutensol AO-10 (BASF AG, Germany) represents the oxyethylated higher fatty alcohols. The structure of Lutensol AO-10 corresponds to the formula $C_n\,H_{2n}{+}1\,O\,(C_2H_4O)_m\,H$, where n is 12–15; m ~10; the mean molecular mass = 654 g mol^{-1} [16].

Macronet MN-200 (Purolite International Ltd.) — a neutral hyper-cross-linked polystyrene adsorbent: thei nner surface area of 1000 m^2/g, a biporous structure (micropores of 1.0–1.5 nm and transport macropores ~100 nm), the specific gravity ~1.04 g/ml, pore volume 1–1.1 ml g^{-1} [17].

Sample of the sorbent was conditioned in methanol-hydrochloric acid mixtures overnight, then washed and kept in distilled water before being used in the sorption experiments. Prior to experiments the sorbent was dried between filter sheets and weighed. Only a wet fraction of narrow size range (0.5–0.7 mm) was used.

The mass of dry sorbent used in calculations of the sorption capacities at equilibrium (q_e) and at time t (q_t) was predetermined dried separate sample of 0.5 g wet sorbent at 60° C for 12 h. The sorption capacities values are presented in mmol per g of dry sorbent.

$CuCl_2$, HCl, NaOH, EDTA disodium salt of analytical grade were purchased from Merck (Germany). The solutions were prepared with freshly distilled water.

2.2. Batch mode adsorption studies

Sorption isotherms and kinetics were determined by the batch method with a shaking speed of 200 rpm. The sorption isotherms were established by the change of the Cu(II) and AO-10 concentrations before and after the contact with Macronet MN-200 in Erlenmeyer flask at 20.0±0.1°C for 7 days, when the adsorption equilibrium was reached. The equilibration time was determined after adsorption studies at various time intervals. Approximately 0.5 g of wet Macronet MN-200 was added to 100 ml of the solution of a given initial concentration in Erlenmeyer flask and equilibrated at shaking. After agitation, samples of 0.2 ml of solution were taken out, and the concentration of Cu(II) or AO-10 and pH determined. A series of experimental solution in the concentration range 1–10 mmol/L AO-10 or Cu(II) were obtained by successive dilution of the stock solutions: 10 mmol L^{-1} AO-10 and $CuCl_2$ one-component solutions and an equimolecular mixture of Cu(II) and AO-10 (10 mmol L^{-1} AO-10 and 10 mmol L^{-1} $CuCl_2$). The pH values of initial solutions were measured and adjusted with 0.1 M HCl to pH 5.3. The value of pH did not alter after sorption. The sorption capacities at equilibrium, q_{eq} (mmol g^{-1}) was calculated by the following equation:

$$q_{eq} = \frac{(C_0 - C)V}{W} \tag{1}$$

Kinetic curves were recorded when the samples of Macronet MN-200 (0.5 g dry mass) were equilibrated with 100 ml of solution at 20.0±0.1°C in Erlenmeyer flask during the predetermined time. Then the samples of test solution (0.2 ml) were withdrawn and the concentration of Cu(II) or AO-10 determined. The initial concentration of AO-10 and $CuCl_2$ was 5 mmol L^{-1} in both one-component solutions and their mixtures. The sorption capacities q_t (mmol g^{-1}) at time t, were calculated by the following equation:

$$q_t = \frac{(C_0 - C_t)V}{W} \tag{2}$$

All experiments were carried out at the initial pH 5.3 in order to prevent precipitation of copper hydroxide (pH 5.7) [15]. Moreover, Macronet MN-200 exhibits cation exchange properties at pH above 3.60 [18].

Cu(II) concentration in solution was determined complexonometrically with 0.1 N of EDTA disodium salt and murexide; the concentration of nonionic surfactant spectrophotometrically using chromazurol S [19]. These methods were tested to be free of cross interferences between both the solutes in the mixtures by measurement of concentration of Cu(II) using atomic adsorption spectrometry (Perkin Elmer 603, USA) at the respective λ_{max} = 324.7 nm and of AO-10 concentration (the chemical oxygen demand) using a Spectroquant TR 320 – Spectroquant Picco analyser (Merck KgaA, Germany).

All experiments were carried out three times. Repetitive measurements showed the reproducibility at the mean relative deviation $\bar{d} / \bar{x} \times 100\% \le 2$ and standard relative deviation $s / \bar{x} \times 100\% \le 2.5$.

2.3. Scanning electron micrography (SEM)

The shapes and surface morphology of resin were measured by using a scanning electron microscope (SEM) EVO 50EP (Carl Zeiss SMT AG), equipped with energy and wave dispersive X-ray spectrometers (Oxford Instruments). The Macronet MN-200 surface morphology was examined with the secondary electrons detector (low vacuum mode, 10 kV, 50 Pa, working distance 10 mm). The elemental composition was determined using sliced specimens coated with carbon. The distribution of Cu(II) in the bead (weight %) was examined with a wave dispersive X-ray spectrometer; X-rays of CuK_a were collected at 16 kV.

3. Results and discussion

3.1. Mutual action of copper (II) and AO-10 on the equilibrium of their sorption by Macronet MN-200

The effect of initial solution concentration on the simultaneous sorption of Cu(II) and AO-10 onto MN-200 was evaluated. As can be seen from Fig. 1, the sorption of AO-10 decreases as the initial copper(II) concentration increases from 2.5 to 10 mmol L^{-1}. Whereas different initial concentrations of AO-10 play different roles in Cu(II) sorption: the maximum q_{eq} of copper(II) was reached at a molar fraction of Cu(II) equal to that of AO-10 (1:1) in the initial mixture. Consequently, further investigations were performed with the molar fraction of solutes 1:1 in the mixtures.

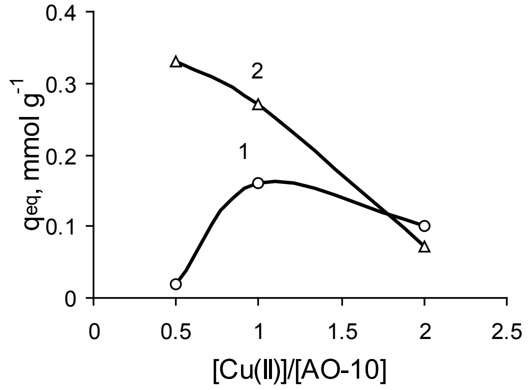

Fig. 1. Sorption isotherms of MN-200 for: copper (II) (1) and AO-10 (2). Initial total concentration of Cu(II) and (AO-10) in mixture = 10 mmol L^{-1}, pH 5.3.

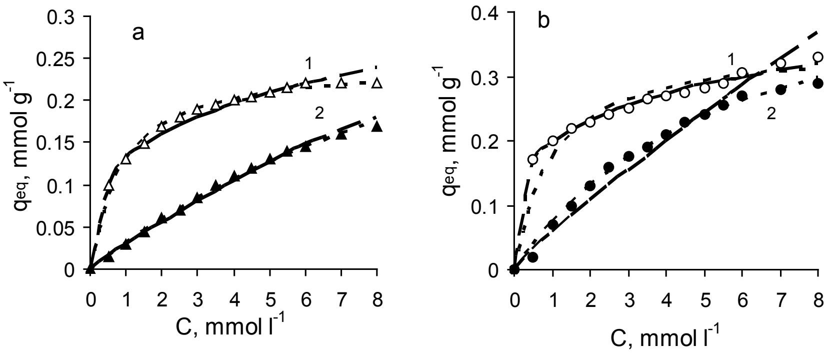

Fig. 2. Sorption isotherms of Macronet MN-200 for (a): 1) Cu(II) without AO-10, 2) Cu(II) in the presence of (AO-10); (b): 1) (AO-10) without Cu(II), 2) (AO-10) in the presence of Cu(II)). - - - calculated after Langmuir [Eq. (3)]; - - - calculated after Freundlich [Eq. (4)].

The equilibrium sorption isotherm was obtained plotting graphically the solid phase concentration versus the liquid phase. Whereas the sorption of Cu(II) in the presence of AO-10 (Fig. 2a) is lower than that without AO-10, similarly to the sorption of AO-10 in the presence of Cu(II) is lower than that without Cu(II) (Fig. 2b). This is because in the presence of Cu(II) and AO-10 in the mixture the sorptive sites are occupied not only by Cu(II) cations but also by AO-10 molecules; besides, some Cu(II) cations and AO-10 molecules exist in the form of associates (cationic complexes) surrounded by the hydrate envelopes (Fig. 3), and therefore they possess a rather complex steric structure [20]. Consequently, a part of sorption sites, residing in small pores, contained in the deeper layers of the sorbent bead, is screened by the above-associates, and therefore remains inaccessible for both the associates and also unassociated Cu(II) and AO-10.

To optimize the efficiency of the system, designed for the simultaneous removal of Cu(II) and the nonionic surfactant from wastewaters, it is important to establish the sorption mechanism. The isotherm equations, relating two main parameters, the sorbate concentrations in sorbent and in solution, were tested for the sorption of Cu(II) without and with AO-10, as well as AO-10 without and with Cu(II). The model equation according to Langmuir (mono-layer sorption) is as follows [21]:

$$q_{eq} = \frac{q_L k_L C}{1 + k_L C} \tag{3}$$

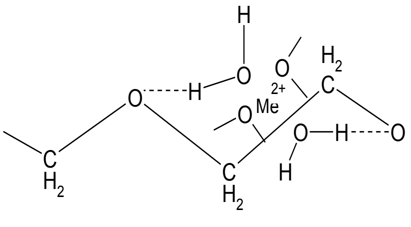

Fig. 3. Structure of the cationic complex [20].

and the model equation according to Freundlich (sorption on a heterogeneous surface) [21]:

$$q_{eq} = k_F C^{1/n} \tag{4}$$

The model Eqs. (3) and (4) can be linearized, leading to Eqs. (5) and (6), respectively [21]:

$$\frac{1}{q_e} = \left(\frac{1}{q_m K_L}\right) \times \frac{1}{C_e} + \frac{1}{q_m} \tag{5}$$

and

$$\ln q_e = \ln K_F + \frac{1}{n} \ln C_e \tag{6}$$

The Langmuir model equation is applicable to the homogeneous adsorption system when there is no interaction between the sorbate molecules, while the Freundlich model is used to describe heterogeneous systems and is not restricted to the formation of the monolayer.

The error, arising from the transformation of the non-linear isotherm equation to the linear form was characterized by both the coefficient of determination (R^2), calculated using the linear regression, and the equivalent mathematical statement (χ^2), calculated after the Chi-square test [22]:

$$\chi^2 = \sum \frac{\left(q_{eq} - q_{eq}^{cal}\right)^2}{q_{eq}^{cal}} \tag{7}$$

where q_{eq}^{cal} is the sorption capacity at equilibrium, calculated from the model chosen (Langmuir or Freundlich) (mmol g^{-1}). An inadequacy of the coefficient R^2 when fitting Langmuir and Freundlich isotherms was mentioned in [22]. The possibility to present for comparison of all the isotherms in the same abscissa–ordinate system is an advantage of the Chi-square test. If the data, calculated using the tested model, corresponded to those, determined experimentally, χ^2 value would be rather low and vice versa.

Constants k_L for the calculation of isotherm according to Langmuir were obtained by plotting C/q_{eq} vs. C (Fig. 4a), and k_F for the calculation of isotherms according to Freundlich — by plotting ln q_{eq} vs. ln C (Fig. 4b). The calculated χ^2 values show better correspondence of the sorption of Cu(II) without and with AO-10 and AO-10 in the presence Cu(II) to the Langmuir model (Table 1) rather than to the Freundlich model (Table 2). The nonionic surfactant molecules with noncyclic poly(oxyethylene) chains are known to form cationic complexes with transition metal ions [20], therefore the formation of multi-layers of adsorbate is not possible due to the electrostatic repulsion between the adsorbed positively charged cationic complexes and those present in the solution (Fig. 3). The isotherms, calculated by the Langmuir model, correspond satisfactorily to those, obtained experimentally (Fig. 2a, Fig. 2b). The experimental qeq value for the sorption of Cu(II) without AO-10 by MN-200 (Figs. 2a, 2b) is comparable with the sorption capacities obtained for H-type granular activated carbon [5], a polyacrylic acid-functionalized cation exchanger (~0.25 mmol g^{-1}) [6], but it is lower than the sorption capacity on fly ash (~0.5 mmol g^{-1}) [23]. Whereas q_{eq} obtained here for AO-10 is similar to that obtained for nonionic surfactants Triton TX-305 and Triton TX-405 sorption onto activated carbon [1]. The sorption capacity of MN-200 (Table 1), determined for AO-10 without Cu (II) is twice as low as that of Purolite C 106 (~1.2 mmol g^{-1}) [6].

The correspondence of the sorption of AO-10 from one-component solution is more adequate to the Freundlich rather than to Langmuir model, and multi-layers of AO-10 can be formed due to the physical interaction of adsorbed AO-10 molecules and those present in the solution. The extent of AO-10 sorption as inferred from

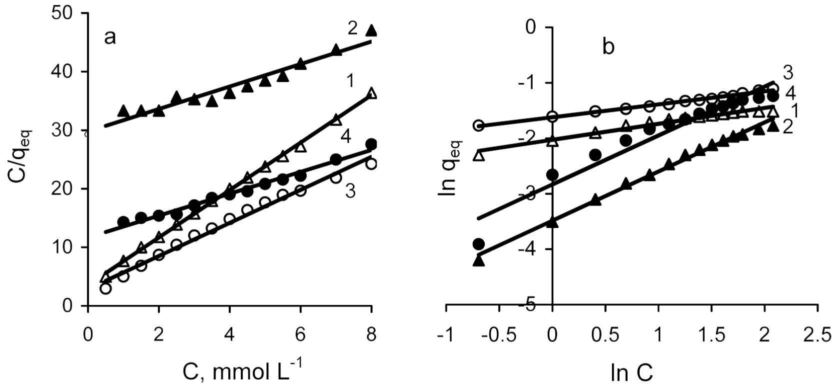

Fig. 4. The plots (a): C/q_{eq} vs. C for the calculation of k_L and q_L after Eq. (3); (b): ln q_{eq} vs. ln C for the calculation of k_F and n after Eq. (4) for sorption: 1) Cu(II) without AO-10; 2) Cu(II) in the presence of AO-10, 3) AO-10 without Cu(II), 4) AO-10 in the presence of Cu(II)).

Table 1
Langmuir constants for copper(II) and Lutensol AO-10 sorption by MN 200, calculated after Eq. (5)

Component	q_{eq} (mmol g^{-1})	k_L (g $mmol^{-1}$)	q_L (mmol g^{-1})	R^2	χ^2
$CuCl_2$	0.21	1.13	0.25	0.9989	0.0017
$CuCl_2$ + (AO-10)	0.13	0.04	0.84	0.9319	0.0011
AO-10	0.28	0.98	0.35	0.9865	0.0329
(AO-10) + $CuCl_2$	0.24	0.16	0.56	0.9831	0.0113

Table 2
Freundlich constants for copper(II) and Lutensol AO-10 sorption by MN 200, calculated after Eq. (6)

Component	k_F (mmol g^{-1})	n	R^2	χ^2
$CuCl_2$	0.13	3.47	0.9641	0.0044
$CuCl_2$ + (AO-10)	0.03	1.13	0.9924	0.0054
AO-10	0.20	4.29	0.9907	0.0012
(AO-10) + $CuCl_2$	0.06	1.13	0.9330	0.0496

the values of K_F calculated for solution free from Cu(II) was higher than that calculated for AO-10 in the presence of Cu(II) or the sorption of Cu(II) from solutions without or with AO-10 (Table 2). The Freundlich constant n values calculated for the sorption of Cu(II) and AO-10 from their mixture are nearer to unity. This implies that the adsorption sites are homogeneous in energy and no interaction between the adsorbed species occurs and the degree of adsorption remained unchanged with changes in the solute concentration [24].The values n for the sorption of Cu(II) without AO-10 and AO-10 without Cu(II) are 3.47 and 4.29, respectively, which shows favorable physical sorption rather than the chemical one [25].

3.2. *Mutual action of copper (II) and AO-10 on the kinetics of their sorption by Macronet MN-200*

Most sorption processes occur by the multistep mechanism, comprising the diffusion across the liquid film surrounding the sorbent particles (process controlled by an external mass transfer), and the diffusion within the particle itself assuming a pore diffusion mechanism (process, controlled by the intraparticle diffusion), and physical or chemical adsorption at a site [26–29].

The time-dependent behavior of Cu(II) and AO-10 sorption from one-component solutions and from their mixtures was examined by varying the contact time between Macronet MN-200 and the solution at the initial pH 5.3. The experimental data obtained were analyzed using the pseudo-second-order rate model. This model was selected because there is no need to determine experimentally the equilibrium capacity, as it can be calculated from the model equation [28]. In addition, the initial sorption rate can also be obtained from the model equation. The linear form of the pseudo second-order kinetic model equation is [28]:

$$\frac{t}{q_t}=\frac{1}{k_2 q_{eq}^2}+\frac{1}{q_{eq}}t \tag{8}$$

k_2 values were determined using the plots t/q_t vs. t for Cu(II) (Fig. 5a) and for AO-10 (Fig. 5b). For Cu(II) the k_2 values obtained are higher than those for AO-10. This could be explained by the different size of the sorbate particles: cations of Cu(II) including their hydrate envelope, are smaller than the molecules of AO-10: the smaller the particle the weaker the hindrance by the backbone of the sorbent against the diffusion, the faster the diffusion. The presence of AO-10 in the mixture results in a decrease in k_2 value for Cu(II), whereas the presence of Cu(II) leads to an increase in k_2 for AO-10 (Table 3). The mutual action of Cu(II) and nonionic surfactant (oxyethylated alcohols) on the rate constants k_2 can be explained as follows: the total surface charge of MN-200, measured as the point

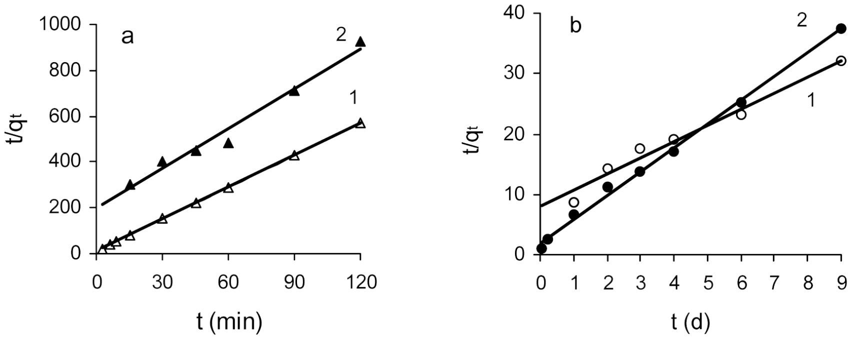

Fig. 5. Plots t/q_t vs. t for the determination of kinetic parameters k_2 and q_{eq} after Eq. (6) characterizing the sorption on MN 200: (a) Cu(II) without AO-10 (1) and Cu(II) in the presence of (AO-10) (2); (b) AO-10 without Cu(II) (1) ad AO-10 in presence Cu(II) (2).

Table 3
Mutual action of copper (II) and AO-10 on kinetic parameters obtained after pseudo-second-order kinetic model. Initial concentration of Cu(II) and (AO-10) — 5 mmol L^{-1} in one-component solution and in mixture

Composition	q_{eq}* (mmol g^{-1})	Parameters for pseudo second order kinetics [Eq (6)]		
		k_2 (g $mmol^{-1}$ h^{-1})	q_{eq} (mmol g^{-1})	R^2
Cu(II)	0.21	110.15	0.21	0.9998
Cu(II) + (AO-10)	0.13	10.34	0.16	0.9758
AO-10	0.28	0.085	0.30	0.9748
(AO-10) + Cu(II)	0.24	0.350	0.25	0.9960

*determined experimentally

of zero charge (pH_{pzc}), was determined previously [18]. The obtained pH_{pzc} value equal to 3.60 is in agreement with the data of Boehm titration: the MN-200 surface displayed a total acidity of 0.2 mmol g^{-1} which contributed only to a high phenolic hydroxyl group concentration of 0.2 mmol g^{-1}. The pHpzc is lower than that of the equilibrium solution pH which is equal to 5.3, indicating the occurrence of a negative charge in the whole net of MN-200 which is important for electrostatic interaction both with Cu(II)cation and with the cationic complexes of Cu(II) cations and AO-10 molecules. It could be the reason for adsorption rate constant k_2 higher for AO-10 with Cu(II) when compared to k_2 for AO-10 without Cu(II).

3.3. *Mutual action of copper (II) and AO-10 on the diffusion mechanism of their sorption by Macronet MN-200*

The pseudo-second order kinetic model cannot describe the diffusion mechanism and therefore the kinetic results were analyzed by using the intraparticle diffusion model. According to this model, the initial rate of intraparticle diffusion is given by Weber–Morris equation [29]:

$$q_t = k_i\left(t^{0.5}\right) + A \tag{9}$$

In theory the plot q_t vs. $t^{0.5}$ is represented by a multiple region, reflecting the external mass transfer, followed by the intraparticle diffusion in macro, meso and micropores [25].

Since the linear dependence of q_t on $t^{0.5}$, inherent to the sorption limited by intraparticle diffusion, is not observed for Cu(II) without or with AO-10 (Fig. 6a) it may be supposed that the sorption is governed by both the intraparticle diffusion and the external mass transfer through the liquid film, surrounding the sorbent bead. Two linear segments, distinguished in the plots q_t vs. $t^{0.5}$, also refer to the two-stage diffusion. The slope of the second linear segment characterizes the rate parameter k_i, corresponding to the intraparticle diffusion. For Cu(II) and for AO-10 sorption from one-component solution the uniform values of k_i are obtained, whereas the value k_i obtained for Cu(II) in the presence of AO-10 is considerably higher than that obtained for AO-10 in the presence of Cu(II) (Table 4). Presumably the diffusion of that part of Cu(II), which enters into the complexes with AO-10 mentioned above, is less interfered with the hydrated Cl- coions than without AO-10. Moreover, a highly developed porosity of MN-200 promotes the intraparticle diffusion of the associates despite their complex steric structure. This could be confirmed by a minor increase in k_i for AO-10 in the presence of Cu(II), which is illustrated by the SEM micrograph in Fig. 8. Upon the SEM micrograph MN-200 is a typical macro network, similar to that of the isoporous styrene Styrosorb type polymers presented in [12]. After saturation with AO-10 the formation of coils of AO-10, hindering the diffusion is observed (Fig. 8b).

The values of intercept *A* in Eq. (9) may be used for indirect characterization of the boundary layer thickness: the greater intercept obtained means a greater boundary layer effect. Whereas the value of the intercept *A* for sorption of Cu(II) in the presence of AO-10 seems to be negative (Fig. 6a second linear segment of curve 2) therefore such characteristic of the boundary layer effect is mindless. Consequently, external mass transfer was characterized using the plot C/C_0 vs. time *t* for contact time up to 15 min. The rate constant k_s (Fig. 6b) shows that the external transfer of Cu(II) in one-component solution is 2.3-fold slower than that in the presence of AO-10 (Table 4).

The linear dependence of q_t on $t^{0.5}$, inherent to the sorption limited by intraparticle diffusion is observed for AO-10 without or with Cu(II) (Fig. 7). However, the plots obtained do not pass through the origin (Fig. 7), which is indicative of inconsiderable degree of boundary layer control. The values of intercept *A* (Table 4) may be used for indirect characterization of the boundary layer thickness: the intercept obtained is greater for sorption

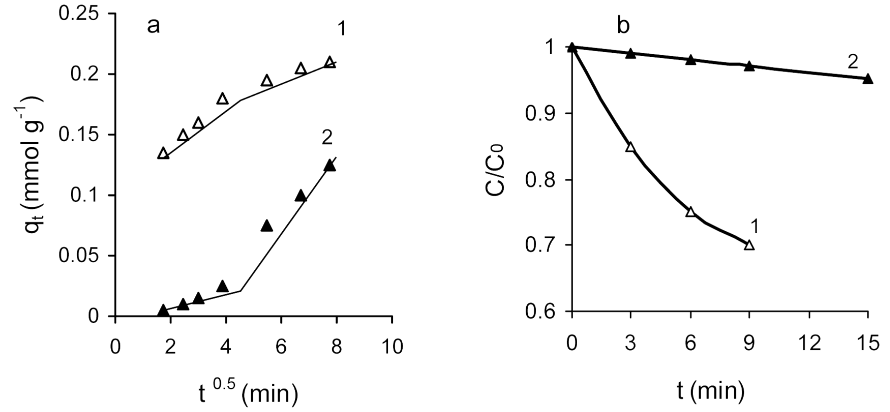

Fig. 6. Plots for the determination of kinetic parameters, characterizing the sorption of Cu(II) without AO-10 (1) and Cu(II) in the presence of AO-10 (2) by MN-200: (a) q_t vs. $t^{0.5}$ — for k_i after Eq. (7); (b) C/C_0 vs. *t* — for k_s.

Table 4
Mutual action of AO-10 and copper(II) on intraparticle and external diffusion. Initial concentration of Cu(II) and (AO-10) — 5 mmol L^{-1} in single component solution and in mixture

Composition	Intraparticle kinetics			External diffusion model	
	k_i (mmol g^{-1} $h^{-0.5}$)	A (mmol g^{-1})	R^2	k_s (h^{-1})	R^2
Cu (II)	0.093		0.9765	0.124	1
Cu (II) + (AO-10)	0.163		0.9735	0.286	0.999
AO-10	0.093	0.0143	0.9896		
(AO-10) + Cu(II)	0.106	0.0342	0.9804		

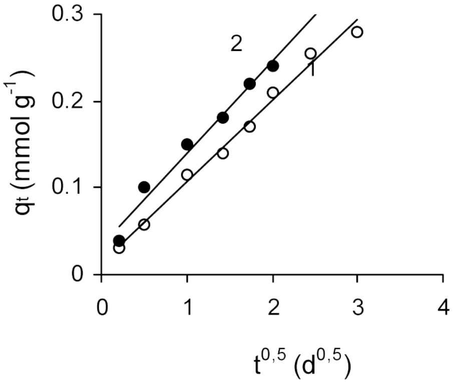

Fig. 7. Plot q_t vs. $t^{0.5}$ for the determination of parameters k_i and A, characterizing the sorption of AO-10 without Cu(II) (1) and AO-10 in the presence of Cu(II) (2) by MN-200.

of AO-10 in the presence of Cu(II) which means a greater boundary layer effect when comparing with that for AO-10 sorption from one-component solution.

To determine the actual rate-controlling step involved in the Cu (II) and AO-10 sorption process, the data obtained were further analyzed after the Boyd plot method [26,29]:

$$\frac{q_t}{q_{eq}} = 1 - \frac{6}{\pi^2}\exp(-Bt) \tag{10}$$

where Bt is the mathematical function of the fraction of the solute sorbed at different times t (q_t/q_{eq}), q_t is the sorption at time t and q_{eq} is the sorption at equilibrium, taken from the second order kinetic model, mmol g^{-1}. From Eq. (10) Bt is derived:

$$Bt = -0.4977 - \ln\left(1 - \frac{q_t}{q_{eq}}\right) \tag{11}$$

Using Eq. (11) Bt value can be calculated for each (q_t/q_{eq}) value. The linearity of this plot should provide information, which allows distinguishing the sorption rate, controlled by the external mass transfer and the rate, controlled by the intraparticle diffusion [29]. The plots Bt vs. t (Fig. 9a) as well as the plots q_t vs. $t^{0.5}$ (Fig. 6a, are not linear, it may be stated that the process, limiting the sorption of Cu(II) from one-component solution or in the presence of AO-10, as it was mentioned above, is governed not only by the intraparticle diffusion, but also by the external mass transfer through the liquid film, surrounding the sorbent bead. Whereas for AO-10 sorption from one-component solution the obtained plots Bt vs. t (Fig. 9b, curve 1) as well as q_t vs. $t^{0.5}$ (Fig. 7 curve 1) are linear, it may be suggested that the process, limiting the sorption of AO-10 from one-component solution is governed by the intraparticle diffusion only, whereas the sorption of AO-10 from the mixture depends on the intraparticle diffusion with an inconsiderable boundary layer effect (Fig. 9b, curve 2).

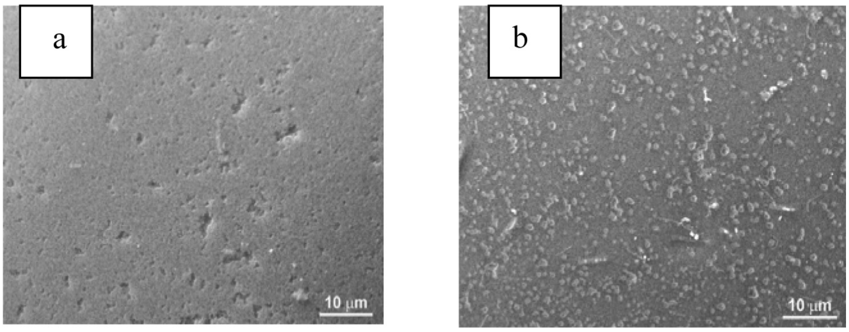

Fig. 8. The SEM micrographs of the MN-200 bead surfaces: (a) after saturation with Cu (II); (b) after saturation with (AO-10).

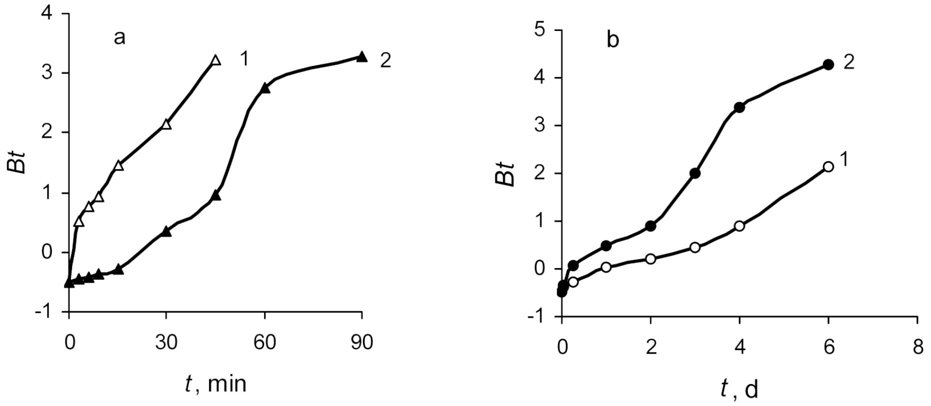

Fig. 9. Kinetics coefficient *Bt* vs. contact time *t* (Boyd plot) characterizing the sorption by MN 200: (a) Cu(II) without AO-10 (1), Cu(II) in the presence of AO-10 (2); (b) AO-10 without Cu(II) (1), AO-10 in the presence of Cu(II) (2).

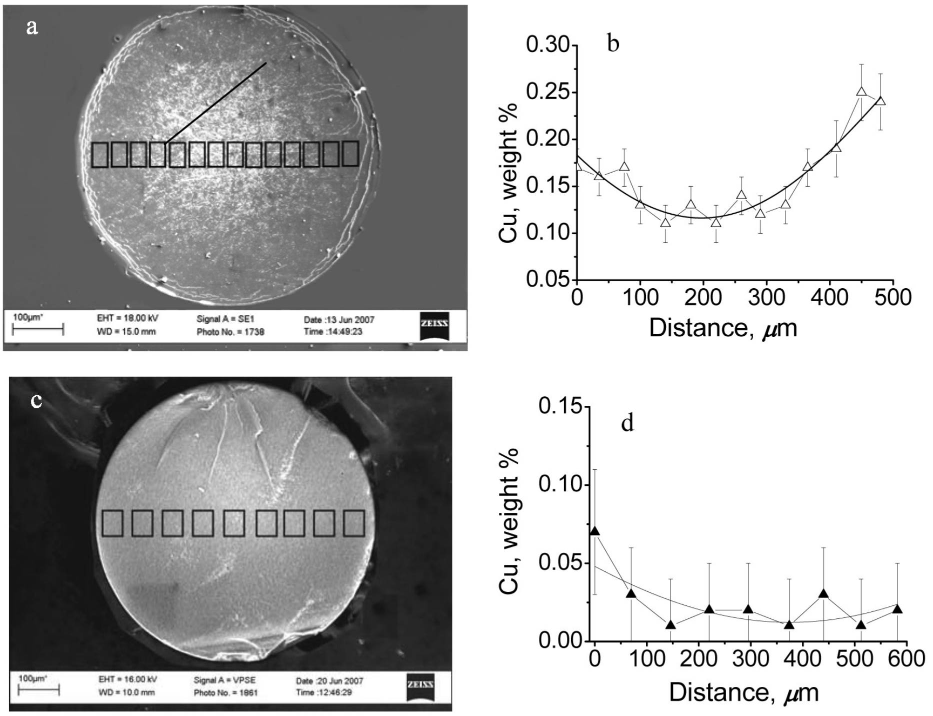

Fig. 10. The SEM micrographs of the cross-section of the MN-200 bead (a), (b): saturated with Cu(II) (5 mmol L^{-1}); (c), (d): saturated with Cu(II) (5 mmol L^{-1}) in the presence of AO-10 (5 mmol L^{-1}).

Fig. 10a and Fig. 10b present SEM micrographs, areas of measurements and distribution of Cu(II) in the cross-section of bead MN-200 saturated with a Cu(II) one-component solution. Fig. 10c and Fig. 10d present SEM photographs, areas of measurements and distribution of Cu(II) in the cross-section of bead MN-200 saturated with a mixture of Cu(II) and AO-10. The minimum Cu(II) concentration is in the center while the maximum concentration is in circumference of bead when MN-200 is saturated with a Cu(II) one-component solution (Fig. 10b). The presence of Lutensol AO-10 in the solution diminishes the sorption of Cu(II) onto MN-200 (Fig. 10d) and the concentration of Cu (II) in the cross-section of the bead is almost constant.

The sorption of Cu(II) and the nonionic surfactant Lutensol AO-10 by Macronet MN-200 is an applicable method for the simultaneous removal of both contaminants from wastewaters, prior to their discharge into effluent, protecting the environment from pollution with cancerous heavy metal compounds and the nonionic surfactant.

4. Conclusions

Simultaneous sorption of copper (II) and nonionic surfactant Lutensol AO-10 (oxyethylated higher fatty alcohols C_nH_{2n}+1O($C_2H_4O_m$H at *n* from 12 to 15, *m* ~10) by Macronet MN-200 (hyper-cross-linked polystyrene) from an aqueous solution results in decrease of the equilibrium sorption (q_{eq}) for both Cu(II) and AO-10 and more homogenous distribution of Cu(II) in the bead of the sorbent. The experimental data showed good correlation with the Langmuir and Freundlich isotherms models. The qeq value calculated using the Langmuir model is greater for AO-10 than that for Cu(II).

The kinetics of the sorption of Cu(II) and Lutensol AO-10 from the one-component solutions and from the mixtures corresponds to the pseudo-second-order kinetic model at the coefficient of determination $R^2 > 0.97$. The kinetic parameters for Cu(II) are higher than those for Lutensol AO-10, whereas the sorption of AO-10 proceeds faster in the presence of Cu(II), than that without copper(II).

The external mass transfer through the liquid film surrounding the bead of MN 200 and intraparticle diffusion of Cu(II) from one-component solution proceeds slower than that of Cu(II) from the mixture with Lutensol AO-10. The intraparticle diffusion of both the Cu(II) and Lutensol AO-10 present in the mixture is promoted by their mutual influence.

Symbols

C_0 — Concentrations of Cu(II) or AO-10 solutions before sorption, mmol L^{-1}
C — Concentrations of Cu (II) or AO-10 solutions after sorption, mmol L^{-1}
V — Volume of solution, L
W — Mass of dry resin, g
q_{eq} — Sorption capacity at equilibrium, mmol g^{-1}
q_t — Sorption capacity at time t, mmol g^{-1}
q_L — Langmuir constant, mmol g^{-1}
k_L — Langmuir constant, g $mmol^{-1}$
k_F — Freundlich constant, mmol g^{-1}
n — Freundlich exponent
q_{eq}^{cal} — Calculated sorption capacity at equilibrium, mmol g^{-1}
k_2 — Pseudo second order rate constant, g $mmol^{-1}$ h^{-1}
k_i — Intraparticle diffusion coefficient, mmol g^{-1} $h^{0.5}$
Bt — Mathematical function of the fraction of the solute sorbed at different times *t*
$\bar{d}/\bar{x}$ — Mean relative deviation $\bar{d}/\bar{x}$, 100%
$s/\bar{x}$ — Standard relative deviation, 100%
χ^2 — Equivalent mathematical statement calculated after Chi-square test

References

[1] C.M. Gonzalez-Garcia, M.L. Gonzalez-Martin, J.F. Gonzalez, E. Sabio, A. Ramiro and J. Ganan, Non-ionic surfactants adsorption onto activated carbon: Influence of the polar chain length, Powder Technol., 148 (2004) 32–37.

[2] J.P. Chen and M. Lin, Nonionic surfactants adsorption onto activated carbon: Influence of the polar chain length, Water Res., 35 (2001) 2385–2394.

[3] J.P. Chen and L. Wang, Characterization of metal adsorption kinetic properties in batch and fixed bed reactors, Chemosphere, 54 (2004) 397–404.

[4] C.Y. Yin, M.K. Aroua and W.M.A. Wan Daud, Review of modifications of activated carbon for enhancing contaminant uptakes from aqueous solutions, Separ. Purif. Technol., 52 (2007) 403–415.

[5] J.P. Chen and Sh. Wu, Simultaneous adsorption of copper ions and humic acid onto activated carbon, J. Colloid Interf. Sci., 280 (2004) 334–342.

[6] D. Kaušpėdienė, J. Snukiškis and A. Gefenienė, Kinetic behaviour of Duolite ES 468 in cosorption of non-ionic surfactant and copper(II), J. Hazard. Mater., 4035 (2003) 1–7.

[7] M.H. Tai, B. Saha and M. Streat, Characterization and sorption performance of a Hypersol-Macronet polymer and an activated carbon, React. Func. Polym., 41 (1999) 149–161.

[8] M.P. Baya, P.A. Siskos and V.A. Davankov, Evaluation of a hypercrosslinked polystyrene, MN-200, as a sorbent for the preconcentration of volative organic compounds in air, J. AOAC Inter., 83 (2000) 579–583.

[9] N.A. Penner, P.N. Nesterenko, M.M. Ilyin, M.P. Tsyurupa and V.A. Davankov, Investigation of the properties of hypercrosslinked polystyrene as a stationary phase for high-performance liquid chromatography, Chromatographia, 50 (1999) 611–620.

[10] M. Streat and L.A. Sweetland, Physical and adsorptive properties of Hypersol-Macronet™ polymers, React. Funct. Polym., 35 (1997) 99–109.

[11] R.M.C. Sutton, S.J. Hill and P. Jones, High-performance chelation ion chromatography for the determination of traces of bismuth in lead by means of a novel hypercrosslinked polystyrene resin, J. Chromatogr. A, 789 (1997) 389–394.

[12] M.P. Tsyurupa, O.G. Tarabaeva, A.V. Pastukhov and V.A. Davankov, Sorption of ions of heavy metals by neutral hypercrosslinked polystyrene, Inter. J. Polym. Mater., 52 (2003) 403–414.

[13] V.A. Davankov, M.P. Tsyurupa and N.N. Alexienko, Selectivity in preparative separation of inorganic electrolytes by size-exclusion chromatography on hypercrosslinked polystyrene and microporous carbons, J. Chromatogr. A, 1100 (2005) 32–39.

[14] E.Yu. Zakharov, B.E. Rebchikov and B.D. D'yakov, Ion Exchanger Installation in Nuclear Industry, Energoatomizdat, Moscow, 1987.

[15] L. Hartinger. Taschenbuch der Abwasserbehandlung für metallverarbeitende Industry. Band 1: Chemie, Carl Hanser Verlag, München – Vien, 1976.

[16] E.D. Schukin, In A. Abramson and E.D. Schukin, eds., Surface Phenomena and Surface Active Agents, Khimiya, Leningrad, 1984 [in Russian].

[17] Technical data of Macronet MN 200. Available from http://www.puroliteUSA.com.

[18] E. Kazlauskienė, D. Kaušpėdienė, A. Gefenienė, A. Selskienė and R. Binkienė, Sorption of chromium complex dye on activated carbon and neutral polymeric adsorbent, Chemija, 20(2) (2009) 69–77.

[19] E.I. Markova, P.A. Petrov, E.K. Ivanova and Y.A. Barbalat, Application of the aliuminium-chromazurol S complex to photometric determination of nonionic surfactants in aqueous solutions, Zh. Anal. Khim., 41 (1986) 553–557.

[20] V.V. Poushkarev, D.I. Trophimov, Physicochemical Pecularities of Water Cleaning from SSAA. Khimiya, Moscow, 1975 (in Russian).

[21] L.S. Chan, W.H. Cheung and G. McKay, Adsorption of acid dyes by bamboo derived activated carbon, Desalination, 218 (2008) 304–312.

[22] Y.-S. Ho, Selection of optimum sorption isotherm, Carbon, 42 (2004) 2113–2130.

[23] S. Wang, T. Terdkiatburana and M.O. Tade, Single and co-adsorption of heavy metals and humic acid on fly ash, Separ. Purif. Technol., 58 (2008) 353–358.

[24] R.P. Schwarzenbach, P.M. Gschwend and D.M. Imboden, Environmental Organic Chemistry. Wiley-Interscience, New York, 1993.

[25] J.Q. Jiang, C. Coopper and S. Ouki, Comparison of modified montmorillonite adsorbents. Part I: Preperation, characterizationand phenol adsorption, Chemosphere, 47 (2002) 711–716.

[26] K.V. Kumar, V. Ramamurthi and S. Sivanesan, Modeling the mechanism involved during the sorption of methylene blue onto fly ash, J. Colloid Interface Sci., 284 (2005) 14–21.

[27] Y.S. Ho and C.C. Chiang, Sorption studies of acid dye by mixed sorbents, Adsorpt. J. Int. Adsorpt. Soc., 7 (2001) 139–147.

[28] Y.S. Ho and G. McKay, Pseudo-second order model for sorption processes, Process Biochem., 34 (1999) 451–465.

[29] V.K. Gupta and I. Ali, Removal of DDD and DDE from wastewater using bagasse fly ash, a sugar industry waste, Water Res., 35 (2001) 33–40.

[30] Sh. Wang and H. Li, Kinetic modeling and mechanism of dye adsorption on unburned carbon, Dyes Pigments, 72(2007) 308–314.